Resveratrol protects against myocardial ischemic injury via the inhibition of NF-κB-dependent inflammation and the enhancement of antioxidant defenses

YUAN HE[1], XINLIN LU[2], TAO CHEN[2], YU YANG[3], JING ZHENG[4], CAN CHEN[2], YUANQI ZHANG[5] and WEI LEI[1,2]

[1]Laboratory of Cardiovascular Diseases, [2]Cardiovascular Medicine Center and [3]Gerontology Center, Affiliated Hospital of Guangdong Medical University, Zhanjiang, Guangdong 524001, P.R. China; [4]Department of Obstetrics and Gynecology, University of Wisconsin-Madison, Madison, WI 53715, USA; [5]Department of Vascular, Thyroid and Breast Surgery, Affiliated Hospital of Guangdong Medical College, Zhanjiang, Guangdong 524001, P.R. China

Received July 30, 2020; Accepted December 21, 2020

DOI: 10.3892/ijmm.2021.4862

Abstract. Resveratrol (RES) is a natural phenol which possesses multiple pharmacological actions. The present study aimed to determine whether RES protects against myocardial ischemic injury in association with the inhibition of NF-κB-dependent inflammation and the enhancement of antioxidant defenses in mice following acute myocardial infarction (AMI). Male C57/BL mice were randomly assigned to 3 groups as follows: The sham-operated (sham) group, AMI + vehicle group and AMI + RES group. Rat H9C2 cells were also used to examine the effects of RES on hypoxia-induced oxidative injury *in vitro*. Redox homeostasis in the mouse myocardium and rat H9C2 cells was determined post-treatment. The mRNA and protein levels of phosphorylated (p-)IκB kinase (p-IKK), p-nuclear factor (NF)-κB p65, interleukin (IL)-1β, IL-6, nerve growth factor (NGF) and insulin-like growth factor-1 (IGF-1) were measured by RT-qPCR and western blot analysis. It was found that RES slightly protected the myocardium against ischemic injury in mice, while it prevented the hypoxia-induced apoptosis of H9C2 cells. RES decreased the production of reactive oxygen species (ROS) and enhanced the activities of superoxide dismutase (SOD), glutathione (GSH) and glutathione peroxidase (GPx). RES also downregulated the protein and/or mRNA levels of p-IKK, p-NF-κB p65, IL-1β, IL-6, NGF and IGF-1 at 7 and 28 days after infarction. On the whole, these data indicate that RES protects the myocardium against ischemic injury in association with the inhibition of oxidative stress and inflammatory responses. Thus, RES has the potential to be used as an adjunctive therapeutic drug for heart diseases.

Correspondence to: Dr Wei Lei, Laboratory of Cardiovascular Diseases, Affiliated Hospital of Guangdong Medical University, 57 South of Renmin Avenue, Xiashan, Zhanjiang, Guangdong 524001, P.R. China
E-mail: leiwei2006@126.com

Dr Can Chen, Cardiovascular Medicine Center, Affiliated Hospital of Guangdong Medical University, 57 South of Renmin Avenue, Xiashan, Zhanjiang, Guangdong 524001, P.R. China
E-mail: chencan21@163.com

Key words: resveratrol, myocardial ischemic injury, oxidative stress, inflammation, NF-κB

Introduction

Myocardial infarction (MI) is one of the leading causes of mortality worldwide. Oxidative stress and inflammation play key roles in the development of MI (1). In ischemic tissues, reactive oxygen species (ROS) activate the redox-sensitive signaling pathways, damaging the cell components containing phospholipids and proteins (2-4). Nuclear factor-κB (NF-κB) is a complex linked to inflammatory responses and is involved in cellular responses to a variety of stimuli such as stress, ROS, cytokines and pathogens (5-7). Signal-induced ubiquitylation and the subsequent degradation of inhibitors of κB (IκBs) is initiated by the activation of IκB kinase (IKK) (8). Once IκBs are degraded, the NF-κB complex translocates to the nucleus to regulate the expression of specific genes that have DNA-binding sites for NF-κB (8). It has been previously reported that the activation of NF-κB triggered by the Toll-like receptor (TLR) pathway mediates early inflammation during myocardial ischemia and reperfusion (9).

Therapy for MI is aimed at defining cardiomyocyte death and improving prognosis. Accumulating evidence has indicated that a number of traditional herbal drugs, such as grape seed proanthocyanidins extract (GSPE), green tea catechins and Scutellaria baicalensis extract (SbE) can protect cardiomyocytes against ischemia and oxidative injury (10). Resveratrol (RES, 3,5,4'-trihydroxy-trans-stilbene) is a type of natural phenol produced by several plants, including grapes, blueberries, raspberries and mulberries. RES has protective potentials to multi-targets related to cardiovascular diseases (11,12). RES is well-known for its antioxidant, anti-inflammatory and anti-aging properties and anti-coronavirus *in vivo* partially

via scavenging radical molecules (13,14). However, to date, the mechanisms through which RES regulates endogenous antioxidants in the ischemic myocardium remain largely unknown. Several lines of evidence have indicated that numerous protective intracellular pathways of RES are associated with the antioxidant response (14-16). Moreover, RES also exerts anti-inflammatory effects in rat hearts subjected to MI and reperfusion by inhibiting TLR4/NF-κB signaling (9). However, NF-κB promotes cell survival and the transcription of various inflammatory cytokines, and thus it may play both beneficial and detrimental roles in cardiac infarct healing and post-MI remodeling. Therefore, it was hypothesized that the cardioprotective effects of RES against myocardial ischemic injury may be mediated via the inhibition of NF-κB.

The present study demonstrated that the administration of RES to mice with acute MI (AMI) and the treatment of H9C2 cells subjected to oxygen-glucose deprivation (OGD) with RES reduced the production of ROS and increased the activities of cellular antioxidant systems, including superoxide dismutase (SOD), glutathione (GSH) and glutathione peroxidase (GPx), but not catalase (CAT). It was found that treatment with RES did not reduce the myocardial infarct size in C57BL/6 mice, but successfully suppressed myocardial cell apoptosis and increased left ventricular systolic pressure (LVSP). More importantly, mice administered with RES exhibited less production of phosphorylated NF-κB p65 (p-NF-κB p65), phosphorylated IKK (p-IKK), interleukin (IL)-1β, IL-6, nerve growth factor (NGF), andinsulin-like growth factor-1 (IGF-1). These observations indicate that RES is a potential adjunctive therapeutic drug for regulating redox homeostasis and inflammatory responses post-MI; however, the effect of long-term administration of RES *in vivo* needs to be further verified.

Materials and methods

Reagents. RES powder, nitrotetrazolium blue chloride (NBT), 2',7'-dichlorofluorescein (DCF) and 4',6-diamidino-2-phenylindole (DAPI) were purchased from Sigma-Aldrich (Merck KGaA). Dulbecco's modification of Eagle's medium (DMEM) and fetal bovine serum (FBS) were purchased from Invitrogen (Thermo Fisher Scientific, Inc. Cell lysis buffer for western blot analysis and immunoprecipitation, the enhanced BCA protein assay kit, Cell Counting Kit-8 (CCK-8), reactive oxygen species assay kit, catalase assay kit, total glutathione assay kit, and glutathione peroxidase assay kit and total superoxide dismutase assay kit were all purchased from the Beyotime Institute of Biotechnology. The Annexin V-FITC apoptosis detection kit was purchased from BD Pharmingen (BD Biosciences). Caspase-3/7/9 antibody (cat. nos. 14220, 12827 and 9508), p-p65 (S536) antibody (cat. no. 3033), p-IKKα/β (Ser176/180) antibody (cat. no. 2697), GAPDH antibody (cat. no. 5174), anti-rabbit IgG (cat. no. 7074) and anti-mouse IgG (cat. no. 7076) were purchased from Cell Signaling Technology, Inc. Antibodies to IL-1β (sc-12742), IL-6 (sc-32296), NGF (sc-32300) and IGF-1 (sc-518040) were purchased from Santa Cruz Biotechnology, Inc. The *In Situ* Cell Death Detection kit was purchased from Roche Applied Science. TRIzol reagent was purchased from Invitrogen (Thermo Fisher Scientific, Inc.). The PrimeScrip RT reagent kit with gDNA Eraser and SYBR Premix Ex Taq (Tli RNase H Plus) were purchased from Takara Bio Inc.

Cell treatment and OGD. Rat H9C2 cardiac myoblasts purchased from the American Type Culture Collection (ATCC) were cultured in low-glucose DMEM supplemented with 10% FBS and maintained in a humidified atmosphere consisting of 5% CO_2 and 95% air at 37˚C. After acquiring 80% confluency, the H9C2 cells were treated without or with 5-40 μM of RES for 24 h, and then subjected to normoxia and OGD. After being washed 3 times with PBS, the H9C2 cells were cultured with serum-free, low-glucose or glucose-deprived DMEM. For OGD, the cells were placed in a 3-gas incubator (Thermo Scientific Forma 3131; Thermo Fisher Scientific, Inc.) at 37˚C containing 1% O_2, 5% CO_2 and 94% N_2.

Cell viability (CCK-8 assay). Cell viability was assayed at 6-48 h following OGD and RES treatment by CCK-8 assay. At the corresponding time point, 100 μl of CCK-8 solution were added to each well. After being incubated at 37˚C for 2 h, the OD value was detected at a 450 nm wavelength using a microplate spectrophotometer (Epoch; BioTek Instruments, Inc.).

Cell apoptosis (Annexin V/PI double-staining assay). H9C2 cells were digested by 0.25% trypsin. The cells ($1x10^5$) were then suspended in binding buffer. Double staining with Annexin V-FITC/PI (BD 556547) was used to detect cell apoptosis byflow cytometry (FCM, BD FACSCanto II).

Establishment of model of AMI. C57BL/6 mice (male, 20 g, 6-8 weeks old) were kept under a controlled temperature (23±2˚C) and humidity (50±5%) with a 12-h light/dark cycle (lights on at 7:00 a.m.) with free access to food and water. After 2 weeks of adaptive feeding, mice were anesthetized with 1% sodium pentobarbital (80 mg/kg) by an intraperitoneal (i.p.) injection, and randomly assigned to 3 experimental groups as follows: i) The sham-operated (sham) group (n=40): Silk was drilled underneath the left anterior descending artery (LAD but not ligated, and the mice then received the vehicle (0.9% NaCl, i.p.); ii) the AMI + vehicle group (n=50): AMI was induced by ligating the LAD, and the successful ligation of the LAD was evidenced by immediate regional cyanosis in the anterior ventricular wall and the apex of the heart with color change >40% of the left ventricle (LV) and confirmed by electrocardiography (ECG), and the mice then received the vehicle (0.9% NaCl, i.p.); iii) the AMI + RES group (n=50): RES (2 mg/kg/day, i.p.) was administered after the LAD ligation. On post-operative days 1, 7 and 28, the mice were sacrificed by decapitation under anesthesia with 1% sodium pentobarbital (80 mg/kg, i.p.), and the hearts were rapidly harvested for analysis. The animal protocols were conducted according to the National Institutes of Health (NIH) Guide for the care and use of animals in laboratory experiments, and with the approval of the Institutional Animal Care and Use Committee of Guangdong Medical University.

Assessment of infarct size. The myocardial infarct area was measured using the NBT staining method as previously

described (17). The ratio of the infarct area mass to ventricle mass was used asa parameter for estimating the myocardial infarct size.

Transmission electron microscopy (TEM). The H9C2 cells and mouse myocardium were routinely processed by fixation in 2.5% glutaraldehyde at pH 7.2, post-fixation in 1% OsO4 in 0.1 M cacodylate buffer, dehydration through an ethanol series, embedding in epoxy resin, sectioning, and post staining with uranyl acetate, and the ultra-thin sections (70 nm) were then transferred into a copper grid for viewing under a transmission electron microscope (JEM-1400; Jeol, Ltd.).

Terminal deoxynucleotidyl transferase dUTP nick end labeling (TUNEL) staining assay. The mouse heart tissues were embedded in optimum cutting temperature compound (OCT). Sections (5-μm-thick) were prepared from the heart tissues and fixed with 4% paraformaldehyde at room temperature for 30 min. The *In Situ* Cell Death Detection kit (Roche Applied Science) was used for TUNEL staining. Briefly, the heart sections were incubated in a 0.1% Triton X-100 solution for 2 min on ice and then incubated with a TUNEL reaction mixture at 37˚C for 30 min. Finally, the sections were incubated with 1 μg/ml DAPI at 37˚C for 15 min and observed using a laser scanning confocal microscope (TCS SP5 II; Leica Microsystems GmbH).

The TUNEL-positive cells and total cells in 5 viewing fields of the heart sections were counted under a 10X objective microscope lens.

Detection of LVSP. On post-operative days 7 and 28, the mice were anesthetized with 1% sodium pentobarbital (80 mg/kg, i.p.). A catheter was inserted into the carotid artery and advanced into the LV, and LVSP was recorded using an acquisition and analysis system (BL-420F; Chengdu Technology and Market Co., Ltd.).

Redox-system assay. The concentrations of total GSH, as well as the activities of total SOD, GPx and CAT were measured using respective kits. All assays were performed following the manufacturer's protocols. The levels of ROS in the myocardium were determined using a previously described method (18). Briefly, the reaction mixture (1 ml) containing Locke's buffer (pH 7.4), 0.2 ml homogenate of myocardium (0.5 mg protein) and 10 μl of DCFH-DA (5 mM) was incubated for 45 min at room temperature, and then measured using a spectrofluorometer (EnSpire; PerkinElmer) with excitation at 484 nm and emission at 530 nm. Finally, ROS production was measured from a DCF-standard curve.

Reverse transcritpion-quantitative PCR (RT-qPCR). Total RNA was extracted from the myocardium using TRIzol reagent following the manufacturer's protocol. The RNA concentration was determined using UV spectrophotometry and integrity was monitored by electrophoresis. The quantified total RNA was used for reverse transcription to synthesize the first strand cDNA using the PrimeScript RT reagent kit with a gDNA Eraser (Perfect Real Time) kit; and qPCR was performed according to the specifications of the SYBR Premix Ex Taq II (Tli RNase H Plus) kit using the LightCycler 480 Real-Time PCR detection System (Roche Diagnostics). In brief, the cycling conditions were as follows: A pre-run at 95˚C for 10 sec, 40 cycles of denaturation at 95˚C for 5 sec, followed by a 60˚C annealing for 25 sec and a 72˚C extension for 15 sec; the melting curve conditions were as follows: 1 Cycle of denaturation at 95˚C for 10 sec, then from 65˚C change to 95˚C with a temperature change rate of 0.5˚C/sec. GAPDH was used as reference to normalize mRNA expression levels of target genes. The qPCR reactions were performed in triplicate. Relative expression levels of mRNAs are expressed as $2^{Cq(calibrator)-Cq(test)}$ (19). The primers used for RT-qPCR are listed in Table I.

Table I. Sequences of primers used for RT-qPCR.

Gene	Primer sequences
GAPDH	Forward: 5'-TGCCCCCATGTTTGTGATG-3'
	Reverse: 5'-TGTGGTCATGAGCCCTTCC-3'
IL-1β	Forward: 5'-CAAATCTCGCAGCAGCACATC-3'
	Reverse: 5'-TGTCCTCATCCTGGAAGGTC-3'
IL-6	Forward: 5'-GAAGTTCCTCTCTGCAAGA-3
	Reverse: 5'-ACAGGTCTGTTGGGAGTG-3'
NGF	Forward: 5'-CTGGACTAAACTTCAGCATTC-3'
	Reverse: 5'-GTCTGGGGTCTACAGTGATG-3'
IGF-1	Forward: 5'-GATGCTCTTCAGTTCGTGTGTG-3'
	Reverse: 5'-TCTCCAGTCTCCTCAGATCAC-3'

Western blot analysis. Mouse myocardium was homogenized in liquid nitrogen, and tissues were then lysed with cell lysis buffer for western blot analysis and immunoprecipitation. The protein concentration was determined using the BCA method. Briefly, proteins (10 μg) were denatured and separated by 10% SDS-PAGE gels and electroblotted onto PVDF membranes. The membranes were blocked with TBS containing 5% skimmed milk and 0.1% Tween-20 for 1 h at room temperature. After washing 3 times, the membranes were incubated with anti-IL-1β (1:200), anti-IL-6 (1:200), anti-NGF (1:400), anti-IGF-1 (1:400), anti-p-NF-κB p65 (1:1,000) and anti-GAPDH (1:1,000) antibodies for at least 16 h at 4˚C. Anti-rabbit/mouse IgG (1:2,000) was incubated with the membranes at room temperature for 1 h as the secondary antibody. Immunoreactions were detected using an electrochemiluminescence (ECL) system according to the manufacturer's instructions. The gray value was calculated using ImageJ analysis software (National Institutes of Health). All protein expression levels were normalized to GAPDH.

Statistical analysis. Data were analyzed using a Student's t-test or one-way analysis of variance (ANOVA) and post-hoc analysis for significance was performed with the Bonferroni method using GraphPad Prism 5.0 (GraphPad Software, Inc.). Data are expressed as the means ± standard error of means (SEM) and a P-value <0.05 was considered to indicate a statistically significant difference, as previously described (20).

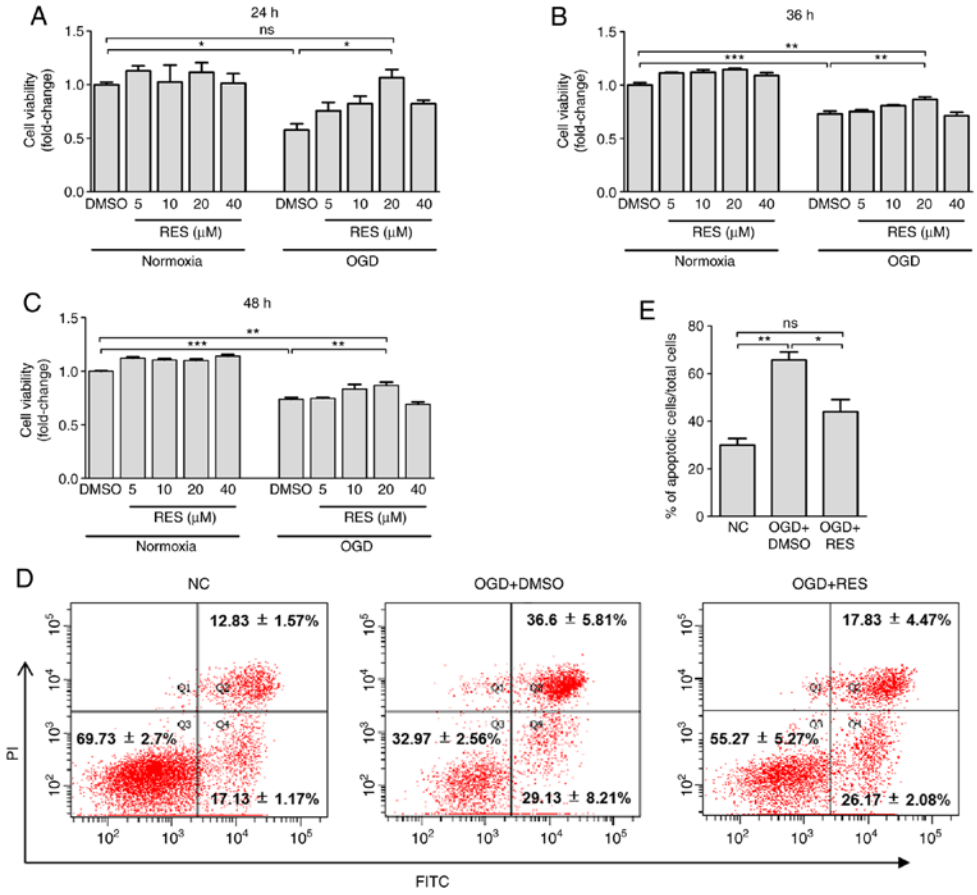

Figure 1. Effect of RES on cell viability and apoptosis. Viability of H9C2 cells was determined by CCK-8 assay at (A) 24 h, (B) 36 h and (C) 48 h after OGD. Apoptosis was detected using FACS. H9C2 cells were exposed to OGD for 24 h and treated with 20 mM RES. The percentages of apoptotic cells were stained by Annexin V-FITC and PI (D). The apoptotic rate was measured by calculating the percentage of early-stage and late-stage apoptotic cells (E). Data are expressed as the means ± SEM (n=3 per group). *P<0.05, **P<0.01, ***P<0.001; ns, not significant. RES, resveratrol; OGD, oxygen-glucose deprivation.

Results

RES promotes H9C2 cell survival and reduces apoptosis. The results of CCK-8 assay revealed that exposure to OGD for 24-48 h incurred a 26-42% decrease in cell viability (Fig. 1A-C). Relative to treatment with DMSO, 20 μM RES significantly increased cell viability by 84.4, 18.6 and 17.5%, respectively at 24, 36 and 48 h post-OGD, while RES at 5 and 40 μM failed to significantly improve cell survival (Fig. 1A-C). However, compared with the normal control (NC) group, non-significant differences in cell viability were observed at 6 and 12 h post-OGD (data not shown). Additionally, as shown by Annexin-V/PI double-staining assay (Fig. 1D and E), exposure to OGD for 24 h significantly increased the numbers of Annexin V^{+}/PI^{+} (late-stage apoptotic) cells. RES significantly decreased OGD-induced cell apoptosis by 33.1%. Taken together, these findings provide strong evidence that RES can protect H9C2 cells against hypoxic injury.

RES attenuates ultrastructural hypoxic changes of H9C2 cells. Electron microscopy examination revealed that the ultrastructure of the NC H9C2 cells was intact. Following exposure to OGD for 24 h, the cell membrane became protruded and foamed, the nuclear membrane cracked, and the nucleolus disappeared in the H9C2 cells (Fig. 2). In the OGD + DMSO group, the cytoplasm was retracted, containing

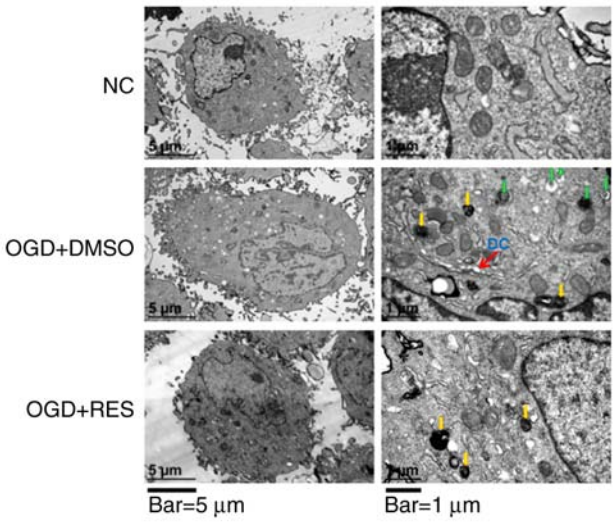

Figure 2. TEM images showing the ultrastructural findings in H9C2 cells. Yellow arrows in the images on the right indicate primary lysosomes. Green arrows in the images on the right indicate autophagic vesicles. DC, dilated cisternae of endoplasmic reticulum. Scale bars, 5 μm (left panels) and 1 μm (right panels). Images were obtained using 2 different magnifications: x8,000 and x30,000. RES, resveratrol; OGD, oxygen-glucose deprivation.

dilated cisternae of endoplasmic reticulum, primary lysosomes and autophagic vesicles (Fig. 2). Treatment of the cells

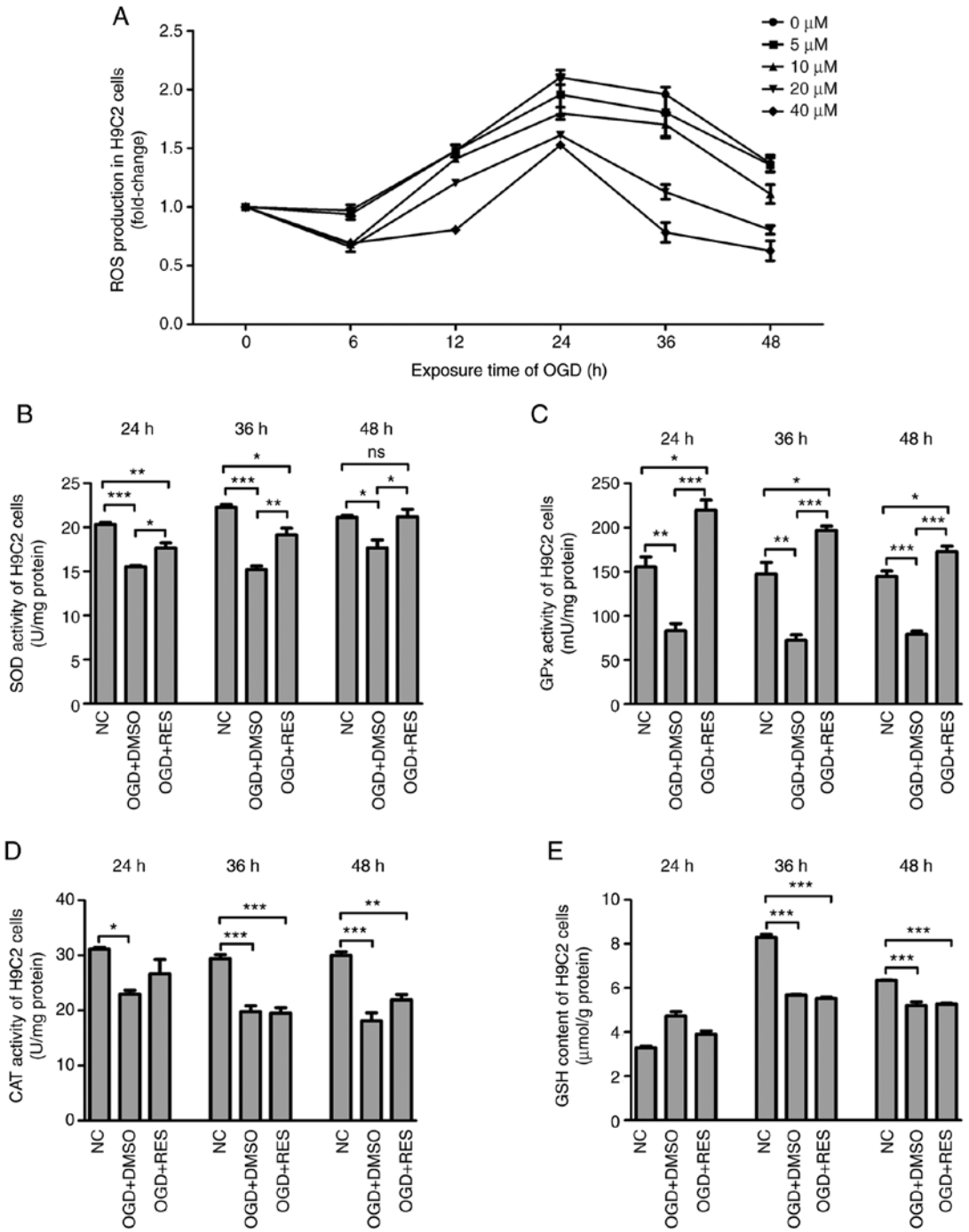

Figure 3. Effects of RES on redox-system of H9C2 cells. (A) ROS production, (B) SOD activities, (C) GPx activities, (D) CAT activities and (E) GSH contents were measured in the H9C2 cells exposed to OGD at different time points. Data are expressed as the means ± SEM (n=3 per group). *P<0.05, **P<0.01, ***P<0.001; ns, not significant. RES, resveratrol; OGD, oxygen-glucose deprivation; ROS, reactive oxygen species; SOD, superoxide dismutase; GPx, glutathione peroxidase.

with RES (20 μM) reduced OGD-induced cell damage, as the cell membrane and nuclear membrane appeared to be intact, autophagic vesicles were reduced and the areas of the cytoplasm became more spacious (Fig. 2). These findings indicate that RES protects cell against ultrastructural damage induced during the earlystages of hypoxia.

RES inhibits hypoxia-induced oxidative stress in H9C2 cells. The effects of RES on ROS production were measured by DCFH fluorescence. It was found that ROS production by the H9C2 cells peaked 24 h following exposure to OGD, and RES decreased ROS generation in a concentration-dependent manner (Fig. 3A). The redox-regulation effect of RES on the antioxidant system in H9C2 cells was also investigated. Compared to the NC group, the level of GSH and the activities of SOD, GPx and CAT in the OGD + DMSO group were significantly decreased. Compared to the OGD + DMSO group, RES increased the activities of SOD and GPx (Fig. 3B and C), but had no effect on CAT activities and GSH contents (Fig. 3D and E). These findings suggest that RES inhibits hypoxia-mediated oxidative stress by scavenging ROS and enhancing endogenous antioxidant systems.

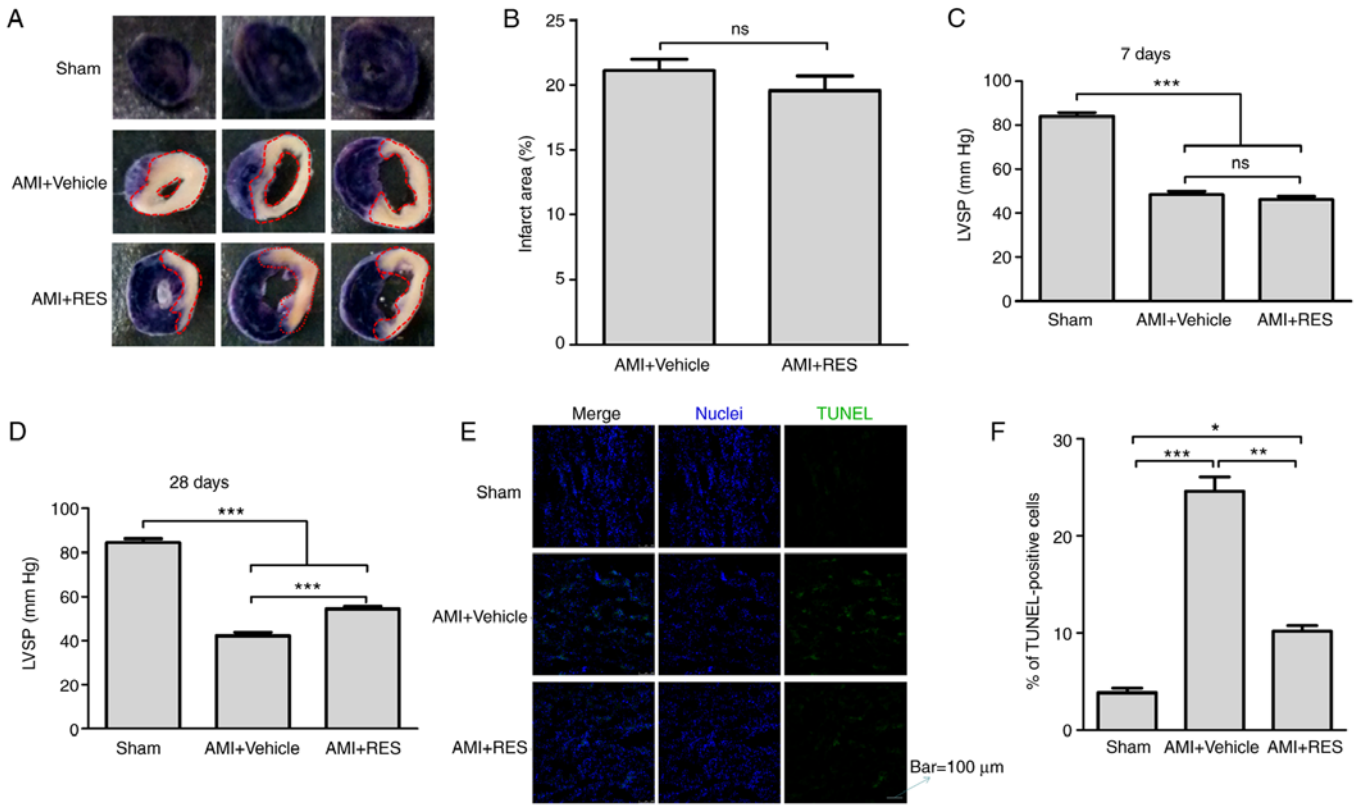

Figure 4. Effects of RES on myocardial infarct size, LVSP and apoptosis in mouse myocardium. (A and B) The myocardial infarct size was measured using the NBT staining method. (C and D) LVSP was recorded using an acquisition and analysis system. (E and F) Apoptosis was assayed by TUNEL staining. Each bar represents the means ± SEM [(B) n=8 per group; (C and D) n=16 per group; (E) n=5 per group]. Scale bar, 100 μm. *P<0.05, **P<0.01, ***P<0.001; ns, not significant. RES, resveratrol; AMI, acute myocardial infarction; LVSP, left ventricular systolic pressure; NBT, nitrotetrazolium blue chloride.

RES does not reduce the myocardial infarct size, but prevents myocardial apoptosis and increases LVSP. The myocardial infarct size was determined using the NBT staining method (Fig. 4A). It was found that the mice with AMI had an infarct area mass of 21.1±0.86% relative to the ventricle mass; however, RES did not decrease the infarct size (Fig. 4B). In addition, the effect of RES on LVSP was examined in order to evaluate the cardiac systolic function post-AMI. As shown in Fig. 4C and D, significant decreases in LVSP were detected in the AMI + vehicle group compared with the sham group (48.5±1.6 vs. 84±1.7 mmHg at 7 days after infarction; 42.2±1.5 vs. 84.6±1.6 mmHg at 28 days after infarction; P<0.001). At 7 days after AMI, no differences were observed in LVSP between the AMI + RES and AMI + vehicle groups (46.1±1.5 vs. 48.5±1.6 mmHg; P>0.05), while at 28 days after AMI, the LVSP in the AMI + RES group (54.4±1.1 mmHg) was significantly higher than that in the AMI + vehicle group (42.2±1.5 mmHg; P<0.001).

Myocardial apoptosis was detected by TUNEL staining. As shown in Fig. 4E, a few apoptotic cells were observed in the sham group. However, the number of apoptotic cells in the AMI+DMSO and AMI + RES groups was greater than that in the sham group. The percentage of apoptotic cells was significantly decreased compared with the AMI + vehicle group (10.3±0.6 vs. 24.6±1.5%; P<0.01; Fig. 4F).

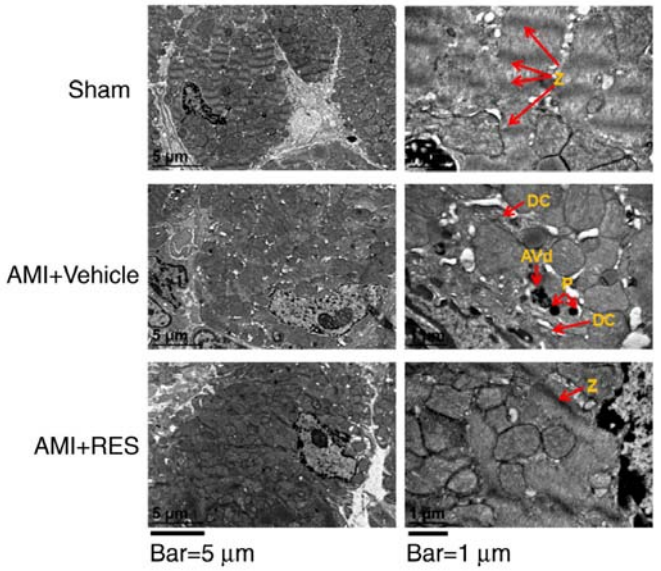

Figure 5. TEM images showing the ultrastructural findings in mouse myocardium. Red arrows labeled with the following indicate: Z, Z lines; DC, dilated cisternae of endoplasmic reticulum; P, primary lysosome; AVd, degradative autophagosomes. Scale bars, 5 μm (left panels) and 1 μm (right panels). Images taken using 2 different magnifications, x8,000 and x30,000. RES, resveratrol; AMI, acute myocardial infarction.

RES attenuates ultrastructural damage due to ischemic injury in the mouse myocardium. In the AMI + vehicle group, the dissolution of myocardial myofilaments, disorganization of substantial sarcomere Z-lines, myofibrillar disarray, dilated

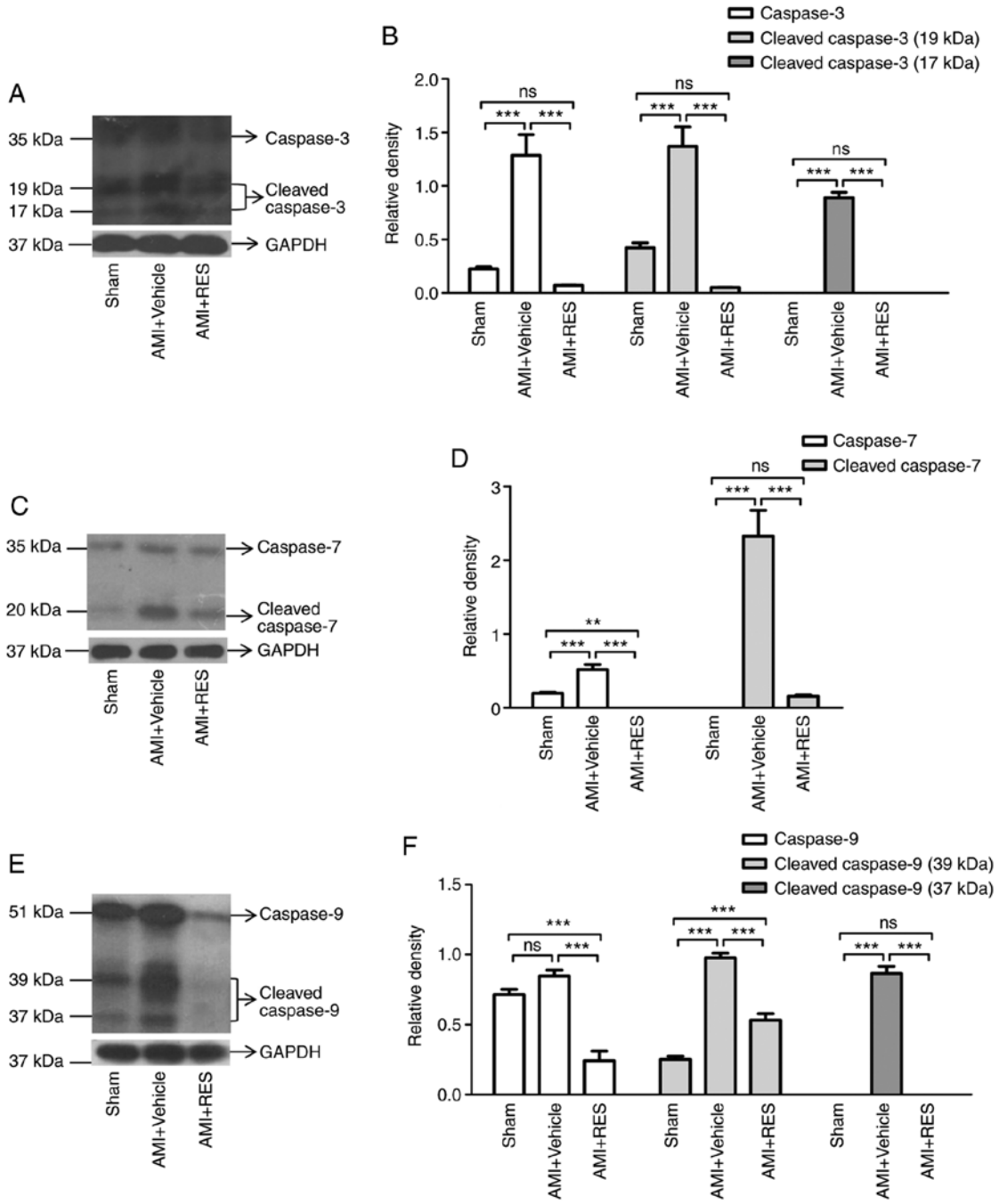

Figure 6. Effects of RES on apoptotic pathways. Expression and cleavage of (A and B) caspase-3, (C and D) caspase-7 and (E and F) caspase-9 in mouse myocardium after ischemia determined by western blot analysis. Data are expressed as the fold change relative to the sham group (n=8 per group). **P<0.01, ***P<0.001; ns, not significant. RES, resveratrol; AMI, acute myocardial infarction.

cisternae of the endoplasmic reticulum, primary lysosomes and autophagic vesicles were observed (Fig. 5). These ultrastructural changes were not observed in the myocardium of the NC and RES-treated AMI mice at 7 days post-infarction (Fig. 5). Collectively, RES alleviated ultrastructural ischemic damage and improved myocardial autophagy.

RES attenuates ischemia-induced caspase-3/7/9 activation in the mouse myocardium. To further confirm whether RES attenuates post-ischemic myocardial apoptosis, western blot analysis was performed to detect the expression and activation of caspase-3/7/9. It was found that the levels of procaspase-3/7/9 and cleaved caspase-3/7/9 were significantly increased in the AMI + vehicle group at 7 days after AMI (Fig. 6). Compared with the AMI + vehicle group, RES treatment significantly decreased the levels of procaspase-3/7/9 and cleaved caspase-3/7/9 (Fig. 6).

RES inhibits ischemia-induced oxidative stress in the mouse myocardium. As shown in Fig. 7A, ROS generation in the AMI + vehicle group was upregulated at 7 and 28 days after AMI. The administration of RES resulted in significantly decreased ROS levels, which were even lower than those of the sham group. As shown in Fig. 7B-D, the levels of GSH,

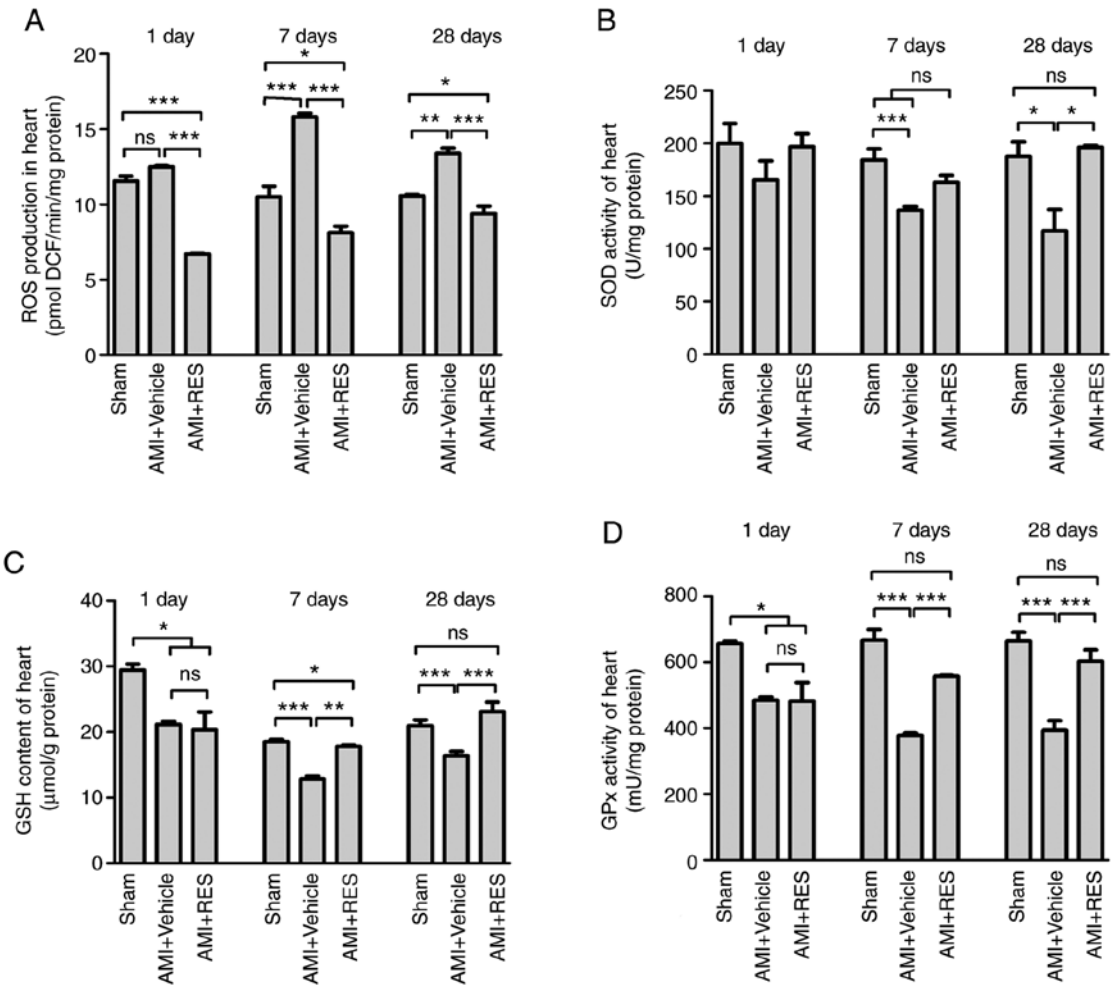

Figure 7. Effects of RES on the redox-system of the mouse myocardium. (A) ROS production, (B) SOD activity, (C) GSH content and (D) GPx activity were measured in the mouse myocardium at 1, 7 and 28 days post-infarction. Data are expressed as the means ± SEM (n=3 per group). *P<0.05, **P<0.01, ***P<0.001; ns, not significant. RES, resveratrol; AMI, acute myocardial infarction; ROS, reactive oxygen species; SOD, superoxide dismutase; GPx, glutathione peroxidase; GSH, glutathione.

and the activities of SOD and GPx decreased post-AMI and RES treatment reversed these effects. These findings further confirmed the antioxidant properties of RES.

RES regulates NF-κB-dependent inflammation. The effects of RES on NF-κB activation and NF-κB-dependent pro-inflammatory pathways were investigated by western blot analysis and RT-qPCR. No significant differences in NF-κB-dependent pro-inflammatory pathways were observed between the sham, AMI + vehicle and AMI + RES groups at 1 day after infarction (data not shown). AMI upregulated the mRNA levels of IL-1β, IL-6, NGF and IGF-1 at 7 and 28 days post-AMI (Fig. 8); however, RES suppressed the mRNA levels of all these peptide factors, apart from NGF. The results of western blot analysis revealed that RES significantly reversed the ischemia-induced elevation of p-IKKα/β, p-NF-κB p65, IL-1β, IL-6, NGF and IGF-1 levels at 7 and 28 days after AMI (Fig. 9). These results imply that RES is an important regulator of NF-κB-dependent inflammation.

The present study demonstrates that RES attenuates oxidative stress and NF-κB-dependent inflammation, and decreases the apoptosis of cardiomyocytes following myocardial hypoxia/ischemia (Fig. 10).

Discussion

Oxidative stress involves an attack on cells when a biological system cannot readily detoxify the redox reactive intermediates or repair the resulting damage. The heart is one of the major organs that is vulnerable to be affected by ROS. Oxidative stress participates in the pathological process of AMI (21). The major ROS include superoxide, hydrogen peroxide (H_2O_2), hydroxyl anions and hydroxyl radicals. H_2O_2, which can freely diffuse across the plasma membrane, is relatively stable under physiological conditions (22). Thus, scavenging H_2O_2 is essential to maintaining redox homeostasis. Superoxide is usually rapidly dismutated to H_2O_2 by SOD. H_2O_2 can be scavenged to H_2O and O_2 by CAT and GPx (23-25).

There is accumulating evidence to indicate that RES not only prevents biomolecule oxidation by being oxidized itself, but also enhances endogenous antioxidant defense system. Recently, Aguilar-Alonso *et al* (26) found that RES treatment decreased the levels of nitric oxide (NO) and malonaldehyde (MDA) in cardiomyocytes during the aging process in rats without significant changes in CAT and SOD levels. The present study demonstrated the antioxidant effects of RES in myocardial ischemic injury. Specifically, the present

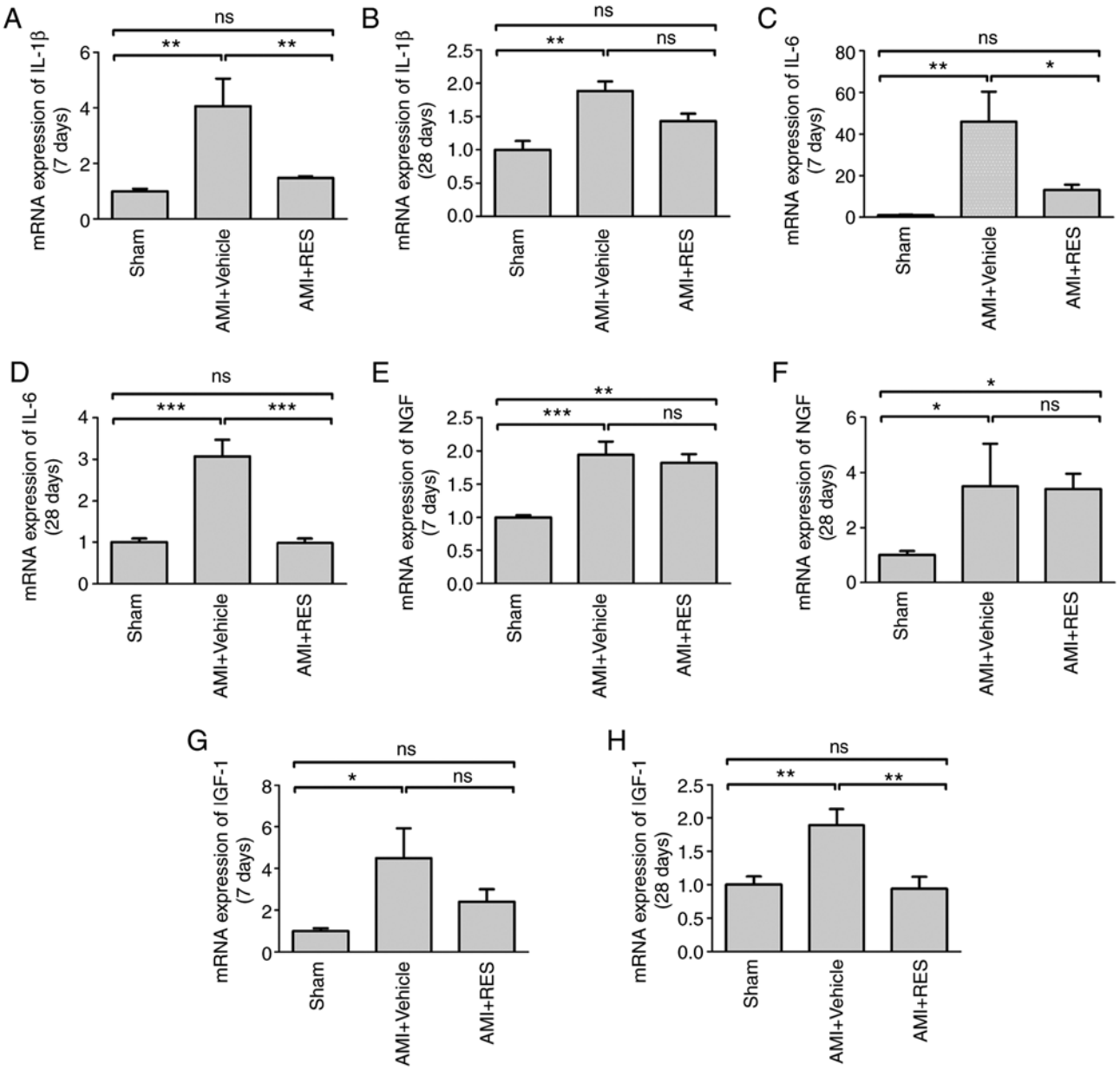

Figure 8. Effects of RES on inflammatory pathways. mRNA levels of (A and B) IL-1β, (C and D) IL-6, (E and F) NGF and (G and H) IGF-1 at 7 and 28 days post-AMI, respectively were measured by RT-qPCR. Data are expressed as the fold change relative to the sham group (n=8 per group). *P<0.05, **P<0.01, ***P<0.001; ns, not significant. RES, resveratrol; AMI, acute myocardial infarction; IL, interleukin; NGF, nerve growth factor; IGF-1, insulin-like growth factor-1.

study demonstrated that RES regulated the production and the balance of ROS in cardiomyocytes (Figs. 1 and 3). The enzyme activities of SOD and GPx, and the GSH content in the mouse myocardium were markedly reduced from the 7th day onward after AMI (Fig. 7), suggesting that the excessive ROS in myocardium may not be scavenged in time. It was found RES exerted protective effects against myocardial ischemic injury in association with enhanced endogenous antioxidant defense systems. These findings suggest that RES may have relatively limited ability to remove H_2O_2.

ROS act as either a signaling molecule or a mediator of inflammation in the infarcted myocardium (27). Inflammation plays a central role in cardiac repair and the pathogenesis of post-infarction remodeling and heart failure (28-31). NF-κB has been identified as a redox-sensitive transcription factor associated with immune responses (2). Upon activation, NF-κB translocates to the nucleus to regulate the transcription of proinflammatory cytokines (32). On the one hand, the increase in the levels of pro-inflammatory cytokines, such as IL-1β and IL-6 induces endothelial cell adhesion molecule synthesis and activates leukocyte integrins, leading to the recruitment of inflammatory cells into the infarcted areas (29), thus aggravating oxidative stress, myocardial infarction and consequent ventricular dysfunction. On the other hand, IL-1β and IL-6 can trigger the expression of growth factors, such as NGF and IGF-1, which promote cardiac repair and preserve cardiac function by preventing negative cardiac remodeling following MI (33-35).

The present study demonstrated that RES treatment inhibited NF-κB signaling pathway activation, and decreased the expression levels of IL-1β, IL-6, NGF and IGF-1 in the myocardium of mice with AMI (Figs. 8 and 9). Moreover, a previous

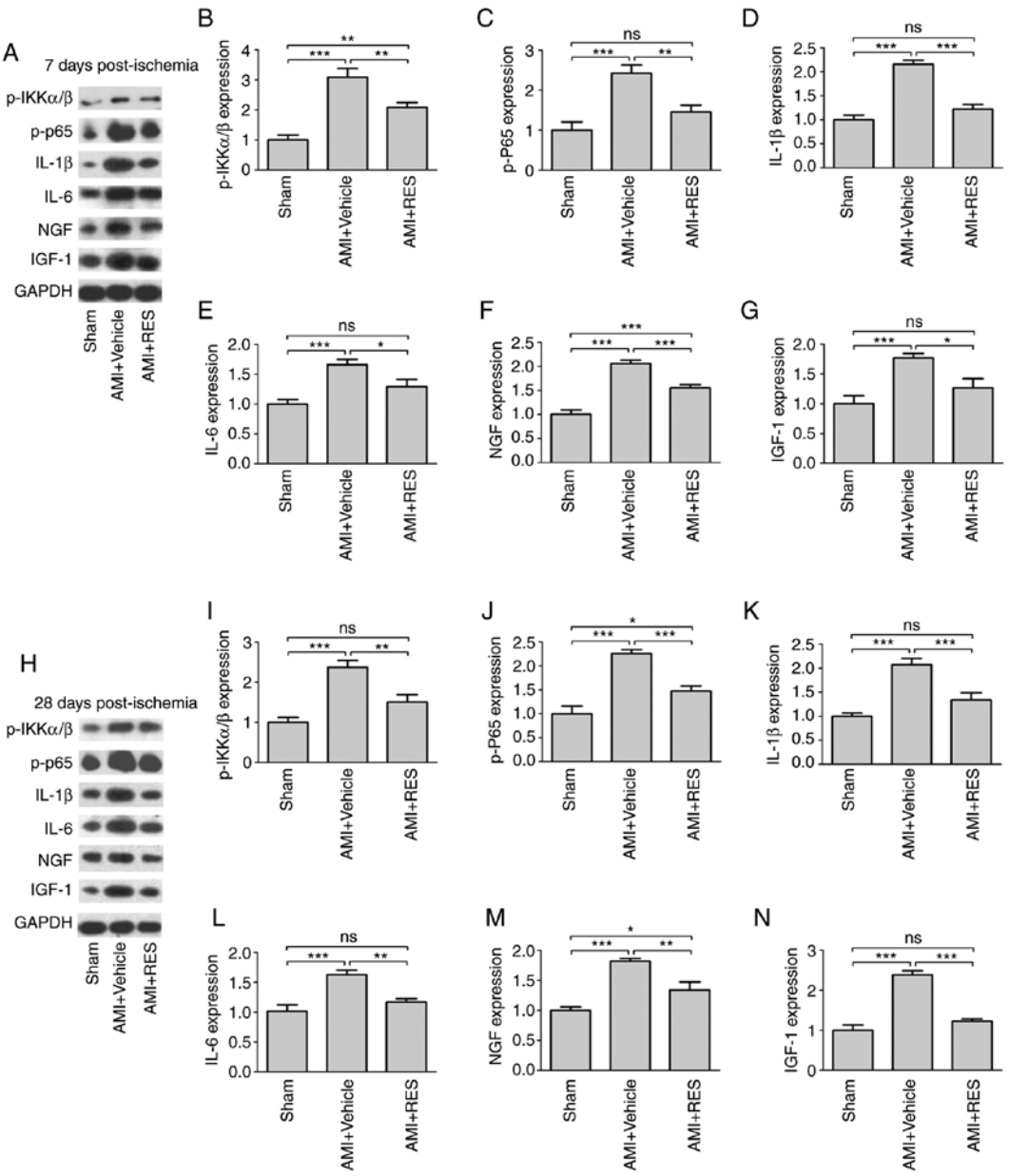

Figure 9. Effects of RES on NF-κB-dependent inflammation. The expression of p-IKKα/β, p-p65, IL-1β, IL-6, NGF and IGF-1 was determined in the mouse myocardium at (A-G) 7 days and (H-N) 28 days by western blot analysis. Data are expressed as the fold change relative to the sham group (n=8 per group). *P<0.05, **P<0.01, ***P<0.001; ns, not significant. RES, resveratrol; AMI, acute myocardial infarction; IL, interleukin; NGF, nerve growth factor; IGF-1, insulin-like growth factor-1.

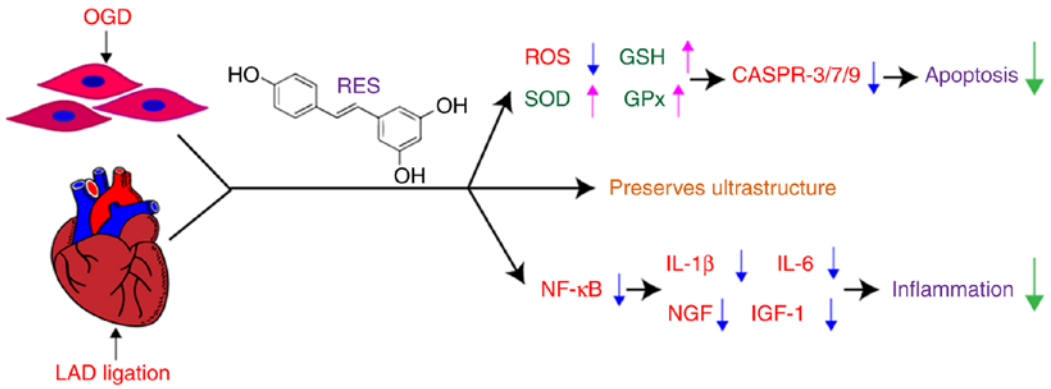

Figure 10. Schematic diagram showing the use of RES to protect against myocardial injury via of inflammation inhibition and antioxidant defenses. OGD, oxygen-glucose deprivation; LAD, left anterior descending branch; RES, resveratrol; ROS, reactive oxygen species; SOD, superoxide dismutase; GSH, glutathione; GPx, glutathione peroxidase; CASPR, caspase.

study by the authors provided evidence that RES attenuated macrophage infiltration in the infarcted zone of the heart (36). Thus, it was hypothesized that RES may have the potential to reverse myocardial fibrosis and pathologic remodeling in the late stage of AMI. Cardiac remodeling has been confirmed to be involved in the pathogenesis and progression of heart failure following MI. Ahmet *et al* (37) found that long-term dietary RES supplementation reduced cardiovascular structural and functional deterioration in chronic heart failure, which verifies our hypothesis.

Multiple lines of compelling evidence indicate that RES possesses antioxidant and anti-inflammatory properties. However, whether antioxidant therapy is a valid means of arresting inflammation in patients remains controversial. Chekalina (38) examined the effect of RES on parameters of central hemodynamics and myocardial ischemia in patients with stable coronary heart disease (CHD), and demonstrated that RES treatment effectively relieved myocardial ischemia and improved LV diastolic function in the patients with CHD. These findingsindicate that RES is applicable for the prevention and therapy of myocardial ischemia. Hence, it is necessary to further explore the long-term effects and underlying mechanisms of RES in patients with AMI.

In conclusion, the present study suggests that RES can potentially be used as a therapeutic and preventive drug for myocardial hypoxic/ischemic injury. However, taking into account the timeliness of RES treatment, it is suggested that optimizing the therapeutic time window of RES against myocardial hypoxic/ischemic injury in patients with CHD may enhance the beneficial effects of RES.

Acknowledgements

Not applicable.

Funding

The present study was supported by the National Natural Science Foundation of China (grant nos. 81700269 and 81970056), the Southern Marine Science and Engineering Guangdong Laboratory Zhanjiang (grant no. ZJW-2019-07), the Natural Science Foundation of Guangdong Province (grant no. 2019A1515011925), the Project of Guangdong Provincial Bureau of Traditional Chinese Medicine (grant no. 20182068), the Competitive Key Scientific and Technological Program of Zhanjiang Municipal Financial Fund (grant no. 2018A01023), and the Stem Cell Preclinical Research Projects of the Affiliated Hospital of Guangdong Medical University (grant no. 2018PSSC004).

Availability of data and materials

All data generated or analyzed during this study are included in this published article or are available from the corresponding author on reasonable request.

Authors' contributions

WL, CC and YZ conceived the study. WL, YH and JZ designed the experiments. YH, XL, TC and YY carried out the experiments and collected the data. YH, JZ and WL wrote and edited the manuscript. All authors read and approved the final manuscript.

Ethics approval and consent to participate

The animal protocols followed the guidelines of the Institutional Animal Care and Use Committee of Guangdong Medical University, and the experiments were conducted according to the National Institutes of Health (NIH) Guide for the care and use of animals in laboratory experiments. The study was approved by the Institutional Animal Care and Use Committee of Guangdong Medical University.

Patient consent for publication

Not applicable.

Competing interests

The authors declare that they have no competing interests.

References

1. Neri M, Fineschi V, Di Paolo M, Pomara C, Riezzo I, Turillazzi E and Cerretani D: Cardiac oxidative stress and inflammatory cytokines response after myocardial infarction. Curr Vasc Pharmacol 13: 26-36, 2015.
2. Morgan MJ and Liu ZG: Crosstalk of reactive oxygen species and NF-κB signaling. Cell Res 21: 103-115, 2011.
3. Pagliaro P and Penna C: Redox signalling and cardioprotection: Translatability and mechanism. Br J Pharmacol 172: 1974-1995, 2015.
4. Hansen JM, Jones DP and Harris C: The redox theory of development. Antioxid Redox Signal 32: 715-740, 2020.
5. Blaser H, Dostert C, Mak TW and Brenner D: TNF and ROS crosstalk in inflammation. Trends Cell Biol 26: 249-261, 2016.
6. Choudhury S, Ghosh S, Gupta P, Mukherjee S and Chattopadhyay S: Inflammation-induced ROS generation causes pancreatic cell death through modulation of Nrf2/NF-κB and SAPK/JNK pathway. Free Radic Res 49: 1371-1383, 2015.
7. Wan J, Shan Y, Fan Y, Fan C, Chen S, Sun J, Zhu L, Qin L, Yu M and Lin Z: NF-κB inhibition attenuates LPS-induced TLR4 activation in monocyte cells. Mol Med Rep 14: 4505-4510, 2016.
8. Hinz M and Scheidereit C: The IκB kinase complex in NF-κB regulation and beyond. EMBO Rep 15: 46-61, 2014.
9. Li J, Xie C, Zhuang J, Li H, Yao Y, Shao C and Wang H: Resveratrol attenuates inflammation in the rat heart subjected to ischemia-reperfusion: Role of the TLR4/NF-κB signaling pathway. Mol Med Rep 11: 1120-1126, 2015.
10. Ahmad R, Javed S and Bhandari U: Antiapoptotic potential of herbal drugs in cardiovascular disorders: An overview. Pharm Biol 48: 358-374, 2010.
11. Bonnefont-Rousselot D: Resveratrol and cardiovascular diseases. Nutrients 8: 250, 2016.
12. Stephan LS, Almeida ED, Markoski MM, Garavaglia J and Marcadenti A: Red wine, resveratrol and atrial fibrillation. Nutrients 9: 1190, 2017.
13. Annunziata G, Sanduzzi Zamparelli M, Santoro C, Ciampaglia R, Stornaiuolo M, Tenore GC, Sanduzzi A and Novellino E: May polyphenols have a role against coronavirus infection? An overview of in vitro evidence. Front Med (Lausanne) 7: 240, 2020.
14. Mao ZJ, Lin H, Hou JW, Zhou Q, Wang Q and Chen YH: A meta-analysis of resveratrol protects against myocardial ischemia/reperfusion injury: Evidence from small animal studies and insight into molecular mechanisms. Oxid Med Cell Longev 2019: 5793867, 2019.
15. Shen X, Wang M, Bi X, Zhang J, Wen S, Fu G and Xia L: Resveratrol prevents endothelial progenitor cells from senescence and reduces the oxidative reaction via PPAR-γ/HO-1 pathways. Mol Med Rep 14: 5528-5534, 2016.

16. Sun ZM, Guan P, Luo LF, Qin LY, Wang N, Zhao YS and Ji ES: Resveratrol protects against CIH-induced myocardial injury by targeting Nrf2 and blocking NLRP3 inflammasome activation. Life Sci 245: 117362, 2020.
17. Ma L, Chuang CC, Weng W, Zhao L, Zheng Y, Zhang J and Zuo L: Paeonol protects rat heart by improving regional blood perfusion during no-reflow. Front Physiol 7: 298, 2016.
18. Shinomol GK and Muralidhara: Differential induction of oxidative impairments in brain regions of male mice following subchronic consumption of Khesari dhal (*Lathyrus sativus*) and detoxified Khesari dhal. Neurotoxicology 28: 798-806, 2007.
19. Livak KJ and Schmittgen TD: Analysis of relative gene expression data using real-time quantitative PCR and the 2(-Delta Delta C(T)) method. Methods 25: 402-408, 2001.
20. Boos DD and Stefanski LA: P-value precision and reproducibility. Am Stat 65: 213-221, 2011.
21. Misra MK, Sarwat M, Bhakuni P, Tuteja R and Tuteja N: Oxidative stress and ischemic myocardial syndromes. Med Sci Monit 15: RA209-RA219, 2009.
22. Bienert GP, Møller AL, Kristiansen KA, Schulz A, Møller IM, Schjoerring JK and Jahn TP: Specific aquaporins facilitate the diffusion of hydrogen peroxide across membranes. J Biol Chem 282: 1183-1192, 2007.
23. Luna CM, Pastori GM, Driscoll S, Groten K, Bernard S and Foyer CH: Drought controls on H_2O_2 accumulation, catalase (CAT) activity and CAT gene expression in wheat. J Exp Bot 56: 417-423, 2005.
24. Bagulho A, Vilas-Boas F, Pena A, Peneda C, Santos FC, Jerónimo A, de Almeida RFM and Real C: The extracellular matrix modulates H_2O_2 degradation and redox signaling in endothelial cells. Redox Biol 6: 454-460, 2015.
25. Rhee SG, Woo HA and Kang D: The role of peroxiredoxins in the transduction of H_2O_2 signals. Antioxid Redox Signal 28: 537-557, 2018.
26. Aguilar-Alonso P, Vera-López O, Brambila-Colombres E, Segura-Badilla O, Avalos-López R, Lazcano-Hernández M and Navarro-Cruz AR: Evaluation of oxidative stress in cardiomyocytes during the aging process in rats treated with resveratrol. Oxid Med Cell Longev 2018: 1390483, 2018.
27. Mittal M, Siddiqui MR, Tran K, Reddy SP and Malik AB: Reactive oxygen species in inflammation and tissue injury. Antioxid Redox Signal 20: 1126-1167, 2014.
28. Frangogiannis NG: Targeting the inflammatory response in healing myocardial infarcts. Curr Med Chem 13: 1877-1893, 2006.
29. Frangogiannis NG: The inflammatory response in myocardial injury, repair, and remodelling. Nat Rev Cardiol 11: 255-265, 2014.
30. Christia P and Frangogiannis NG: Targeting inflammatory pathways in myocardial infarction. Eur J Clin Invest 43: 986-995, 2013.
31. Anzai T: Inflammatory mechanisms of cardiovascular remodeling. Circ J 82: 629-635, 2018.
32. Zhang L, Chen Y, Yue Z, He Y, Zou J, Chen S, Liu M, Chen X, Liu Z, Liu X, *et al*: The p65 subunit of NF-κB involves in RIP140-mediated inflammatory and metabolic dysregulation in cardiomyocytes. Arch Biochem Biophys 554: 22-27, 2014.
33. Mahmoud AI, O'Meara CC, Gemberling M, Zhao L, Bryant DM, Zheng R, Gannon JB, Cai L, Choi WY, Egnaczyk GF, *et al*: Nerves regulate cardiomyocyte proliferation and heart regeneration. Dev Cell 34: 387-399, 2015.
34. Liu Y and Wu JH: GW26-e0203 effects of nerve growth factor on late reperfusion after myocardial infarction. J Am Coll Cardiol 66 (16 Suppl): C28-C29, 2015.
35. Jackson R, Tilokee EL, Latham N, Mount S, Rafatian G, Strydhorst J, Ye B, Boodhwani M, Chan V, Ruel M, *et al*: Paracrine engineering of human cardiac stem cells with insulin-like growth factor 1 enhances myocardial repair. J Am Heart Assoc 4: e002104, 2015.
36. Xin P, Pan Y, Zhu W, Huang S, Wei M and Chen C: Favorable effects of resveratrol on sympathetic neural remodeling in rats following myocardial infarction. Eur J Pharmacol 649: 293-300, 2010.
37. Ahmet I, Tae HJ, Lakatta EG and Talan M: Long-term low dose dietary resveratrol supplement reduces cardiovascular structural and functional deterioration in chronic heart failure in rats. Can J Physiol Pharmacol 95: 268-274, 2017.
38. Chekalina NI: Resveratrol has a positive effect on parameters of central hemodynamics and myocardial ischemia in patients with stable coronary heart disease. Wiad Lek 70: 286-291, 2017.